HGT

In Vivo Potency Testing of Subretinal rAAV5.hCNGB1 Gene Therapy in the *Cngb1* Knockout Mouse Model of Retinitis Pigmentosa

Johanna E. Wagner,[1,†] Lena Zobel,[1,2,†] Maximilian J. Gerhardt,[2] Catherine R. O'Riordan,[3] Amy Frederick,[3] Simon M. Petersen-Jones,[4] Martin Biel,[1] and Stylianos Michalakis[1,2,i,*]

[1]Department of Pharmacy—Center for Drug Research, Ludwig-Maximilians-Universität München, Munich, Germany; [2]Department of Ophthalmology, University Hospital, LMU Munich, Munich, Germany; [3]Gene Therapy, Rare Diseases, Sanofi, Framingham, Massachusetts, USA; and [4]Veterinary Medical Center, Michigan State University, East Lansing, Michigan, USA.

[†]These authors contributed equally to this work and are considered to be co-first authors.

[i]ORCID ID (https://orcid.org/0000-0001-5092-9238).

Retinitis pigmentosa type 45 (RP45) is an autosomal-recessively inherited blinding disease caused by mutations in the cyclic nucleotide-gated channel subunit beta 1 (*CNGB1*) gene. In this study, we developed and tested a novel gene supplementation therapy suitable for clinical translation. To this end, we designed a recombinant adeno-associated virus (rAAV) vector carrying a genome that features a novel human rhodopsin promoter (hRHO194) driving rod-specific expression of full-length human *CNGB1* (rAAV5.hCNGB1). rAAV5.hCNGB1 was evaluated for efficacy in the *Cngb1* knockout (*Cngb1*$^{-/-}$) mouse model of RP45. In particular, increasing doses of rAAV5.hCNGB1 were delivered through single subretinal injection in 4-week-old *Cngb1*$^{-/-}$ mice and the treatment effect was assessed over a follow-up period of 9 months at the level of (1) retinal morphology, (2) retinal function, (3) vision-guided behavior, and (4) transgene expression. We found that subretinal treatment with rAAV5.hCNGB1 resulted in efficient expression of the human CNGB1 protein in mouse rods and was able to normalize the expression of the endogenous mouse CNGA1 subunit, which together with CNGB1 forms the native heterotetrameric cyclic guanosine monophosphate-gated cation channel in rod photoreceptors. The treatment led to a dose-dependent recovery of rod photoreceptor-driven function and preservation of retinal morphology in *Cngb1*$^{-/-}$ mice. In summary, these results demonstrate the efficacy of *hCNGB1* gene supplementation therapy in the *Cngb1*$^{-/-}$ mouse model of RP45 and support the translation of this approach toward future clinical application.

Keywords: adeno-associated virus, AAV, retinal gene therapy, retinitis pigmentosa, CNGB1

INTRODUCTION

Biallelic mutations in the cyclic nucleotide-gated channel subunit beta 1 (*CNGB1*) gene cause a slowly progressing form of retinitis pigmentosa (RP) accounting for ~1% of autosomal recessive RP cases.[1–3] *CNGB1* encodes the beta subunit of the rod-specific cyclic nucleotide-gated channel, which together with the alpha subunit (encoded by *CNGA1*) forms the cyclic guanosine monophosphate (cGMP)-gated cation channel, which localizes to the rod photoreceptor outer segment (OS) plasma membrane and translates light-mediated changes in the second messenger cGMP into voltage and calcium signals.[4] Mutations in *CNGB1* result in rod cyclic nucleotide-gated (CNG) channel deficiency, because of impaired rod CNG channel formation and/or insufficient transport into the OS.[5] The resulting lack of rod channel function leads to loss of rod function, structural defects, and subsequent photoreceptor degeneration[4,6–8] with a classical RP manifestation.[2,9] Clinically, *CNGB1*-linked RP manifests with early-onset night blindness because of decreased rod-mediated function.[2,9] After the third or fourth decade of life and with more progressed rod degeneration, cone photoreceptors start to degenerate secondary to rods, resulting in constriction of peripheral vision and decline of daylight vision.[2,9]

Although no treatment for *CNGB1*-linked RP is yet available, several animal models of *CNGB1*-linked RP have been established[5–7] and facilitated preclinical testing of gene therapy approaches. Previous studies demonstrated that recombinant AAV (rAAV)-mediated supple-

*Correspondence: Prof. Dr. Stylianos Michalakis, Department of Ophthalmology, University Hospital, LMU Munich, Mathildenstr. 8, Munich 80336, Germany. E-mail: michalakis@lmu.de

DOI: 10.1089/hum.2021.121

mentation of murine *Cngb1* to the rods of *Cngb1* knockout ($Cngb1^{-/-}$) mice results in deceleration of disease progression.[10] Likewise, rAAV gene supplementation of canine *Cngb1* in *Cngb1*-deficient dogs resulted in sustained rescue of rod function and preservation of retinal structure.[9]

Here, we developed the novel rAAV vector rAAV5 .hCNGB1 for specific and efficient expression of human *CNGB1* in rods and tested its trans-species potency in treating the RP phenotype in the $Cngb1^{-/-}$ mouse model.[5] In this $Cngb1^{-/-}$ mouse model, rods start to degenerate already at postnatal day 15, resulting in markedly shortened OS at the age of 4 weeks followed by gradual loss of rod cells.[5,9] Cone photoreceptors start to degenerate at the age of 6 months when ~50% of the rods have already been lost. At ~1 year, only 10–20% of the photoreceptors remain.[5] When delivered through single subretinal injection in 4-week-old $Cngb1^{-/-}$ mice, rAAV5.hCNGB1 resulted in improvements in rod function and rod-dependent vision and slowed the rate of retinal degeneration. These therapeutic effects of *hCNGB1* gene supplementation persisted until the end of the observation period of 9 months and hold promise for future translation of this vector into clinics.

MATERIALS AND METHODS

Animals

$Cngb1^{-/-}$ mice[5] were used for testing rAAV5.hCNGB1 and wherever appropriate corresponding *Cngb1* wild-type mice ($Cngb1^{+/+}$) as wild-type controls. The mice were bred on a genetically mixed background of the strains 129/SvJ and C57-Bl6/N, without the *rd8* (*Crb1*[11]) mutation. Mice received food and water *ad libitum* and were maintained in a 12 h light/dark cycle following local regulations and legal guidelines. Animal procedures were approved by the local authority (Regierung von Oberbayern) and were in accordance with the ARVO Statement for the Use of Animals in Ophthalmic and Vision Research.

Cloning and production of rAAV vectors

Standard cloning techniques were used for vector assembly. All sequence manipulations were verified by sequencing. The full-length transcript variant 1 of hCNGB1 (NM_001297.4; 3.75 kb) was PCR amplified[12] and cloned between the inverted terminal repeats (ITRs) of serotype 2 originating from the pSub201 cis-plasmid (131 bp each)[13] together with a short *hRHO* promoter (*hRHO194*; 194 bp), which was PCR amplified from full-length *hRHO* promoter[14] (primer forward 5′-CAT AGC TAG CTT AAG CCT CTC CTC CCT GAC CTC AG-3′ and reverse 5′-TCA TGG ATC CAC TAG TGA TGA CTC TGG GTT CTG ACC-3′). In addition, a previously used short polyadenylation signal (221 bp)[10] acting as an effective termination and polyadenylation enhancer[15] was used. The plasmid backbone contained a pUC18 (Clontech Laboratories, Mountain View, CA) origin of replication, a kanamycin resistance gene (KanR), and randomized synthetic DNA fragments (resulting in the pGL2.0 backbone[14]). The size of the designed vector construct was 4.66 kb from 5′ITR to 3′ITR and thus did not exceed the packaging capacity of rAAV vectors. AAV serotype 5 (AAV5) was used for packaging of this viral genome. The vector was produced by Sanofi Genzyme (Framingham, MA) and was manufactured using a producer cell line based on HeLaS3 cells (ATCC CCL-2.2) as described elsewhere[16] and afterward purified by two-column vector purification using an AVB Sepharose HP column (GE Healthcare) followed by anion exchange chromatography.[17] Virus particle concentration ($\sim 1 \times 10^{13}$ vector genomes (vg) mL^{-1}) was determined by TaqMan PCR assay.[18] Balance salt solution (BSS) +0.014% Tween-20 was used for formulation and vector dilution.

Subretinal injections

Mice were anesthetized by intraperitoneal injection of ketamine (100 mg/kg; Medistar GmbH, Ascheberg, Germany) and xylazine (10 mg/kg, Xylariem®; Ecuphar GmbH, Greifswald, Germany) and pupils were dilated by tropicamide eye drops (Mydriaticum Stulln, Pharma Stulln GmbH, Stulln, Germany). One microliter of diluted viral particles at the indicated dose was slowly injected into the subretinal space using a 34-gauge beveled needle manually operated with a NanoFil syringe (World Precision Instruments, Sarasota, Fl). The process was monitored under a surgical microscope (OPMI 1 FR Pro, Zeiss, Oberkochen, Germany). An injection was considered successful if the formation of a bleb was visible indicating a temporal subretinal detachment of the retina. To confirm the observed result, fundus and retinal monitoring was performed by spectral-domain optical coherence tomography (SD-OCT).[19] After the procedure, all injected eyes were treated with dexamethasone and gentamicin ophthalmic ointment (Dexamytrex®; Bausch and Lomb, Berlin, Germany) for prevention of infection and for eye moisturization.

Electroretinography

Full-field electroretinography (ERG) measurements were performed using the Celeris Fullfield ERG (Diagnosys LLC, Lowell, MA). ERGs were measured under scotopic (dark-adapted) conditions to assess rod-dominated activity. The animals were dark adapted overnight (>12 h) before the measurements. Before the ERG, animals were sedated, and pupils dilated as describe before.[20] Eyes were prevented from drying using methylcellulose (Methocel® 2%; OmniVision), which also provides the corneal contact to the electrode of the Celeris Fullfield ERG. Flashes of varying luminance were directed toward the eyes and the responses were recorded by the ERG device. For single-flash measurements, seven different stimuli from 0.01 to 10 cd s m^{-2} were used (see hereunder) based on the International Society for Clinical Electrophysiology of Vision (ISCEV) standardized protocol for clinical dark-adapted

ERG recordings.[21] All eyes received dexpanthenol eye and nose ointment (Bepanthen®; Bayer) after measurements. Data were analyzed by the Espion software V6.59.9 (Diagnosys LLC).

Spectral-domain optical coherence tomography

SD-OCT measurements were performed using an adapted Spectralis™ HRA+OCT diagnostic imaging platform (Heidelberg Engineering, Dossenheim, Germany) in combination with optic lenses as described previously.[19,20] After sedation and dilatation of pupils as described previously, mice were placed on a platform. The eye to be measured received one drop of methylcellulose (Methocel 2%; OmniVision) and a corneal contact lens before the measurement. OCT scans were obtained using a 12° circular scan mode. Data were analyzed by Heidelberg Eye explorer software V1.7.0.0 (Heidelberg Engineering). OCT scans of each mouse eye were performed directly after the subretinal injections to obtain information about the location of the injection site. The area of each eye that was within the subretinal bleb was used for OCT analysis. For comparison of treated and sham-injected eyes, only OCT scans that had the same distance from the optical nerve were used.

Visual water maze

A modified Morris water maze was previously implemented as a test for vision-guided behavior.[10] In brief, mice had to locate a visible floating platform (10 cm in diameter) in a circular swimming pool (120 cm in diameter, 70 cm high, white plastic; TSE systems, Bad Homburg, Germany). The water was made opaque by the addition of nontoxic white dye to increase visibility of the floating platform. No additional environmental cues were provided. The swimming route of each mouse was tracked using the VideoMot2 software by TSE systems. The experiment was performed on two consecutive days under dim light conditions of 0.32 cd m^{-2} (red light; luminance was determined using the LS-100 luminance meter by Minolta, Marunouchi, Japan) to observe rod-mediated vision-guided behavior. Each time mice were predark adapted for at least 12 h. To test for mainly cone-mediated daylight vision, mice were then tested for another day under bright light conditions (82.8 cd m^{-2}). Each testing day consisted of six trials and starting positions was changed pseudo-randomly on each of the trials. On the different test days, the platform was placed on a new position. One trial ended if the mouse climbed onto the platform or (if the mouse did not find the platform) after 120 s. In the latter case, the mouse was gently placed onto the platform. After each trial, the mouse was allowed to sit undisturbed (for 10 s) on the platform before being removed, placed under a heating lamp, and then transferred to its home cage. The experiment was performed and analyzed blinded to the animal's genotype.

Immunohistochemistry

Immunohistochemical staining was performed after termination of the in-life phase at 9 months postinjection and following previously described procedures.[20,22,23] All animals used for OCT were analyzed. We used the following primary antibodies: rabbit anti-cone arrestin (1:300)[24]; sheep anti-cGMP (1:3,000; Dr. HWM Steinbusch, Maastricht University Medical Center[25]); Cy3-coupled anti-GFAP #C9205 (1:1,000)[22]; rabbit anti-CNGB1 #HPA039159 (1:2,000; Sigma-Aldrich); and rabbit anti-CNGA1 (1:2,000), custom-made against the 19-mer Cys-RLTKVEKFLKPL IDTEFS-HN2, corresponding to 727–744 of human CNGA1 (NP_001136036.1). Laser scanning confocal micrographs were taken using a Leica SP8 confocal system (Leica, Wetzlar, Germany) equipped with the following lasers: 405, 448, 514, and 552 nm. Images were acquired as confocal z stacks using LAS X software V3.5.1.18803 (Leica) and deconvolved by the Huygens Essential software suite V18.04.0p8 64b (Scientific Volume Imaging B.V., the Netherlands) using a signal-to-noise ratio of 5. Maximum projection (merging of all z stacks) and background subtraction (value of 30) was performed using Fiji ImageJ V2.1.0/1.53c software.

Statistics

Statistical significance was evaluated by GraphPad Prism software (version 8 and 9). As statistical tests, either paired or unpaired two-way analysis of variance tests were performed followed by Sidak's *post hoc* test for multiple comparison. All values are given as mean ± standard error of the mean. n is the number of independent measurements and measured values of $p \leq 0.05$ were considered significant. It is defined precisely as follows: $*p \leq 0.05$, $**p < 0.01$, $***p < 0.001$.

RESULTS

Novel short human rhodopsin promoter drives efficient and specific transgene expression in rod photoreceptors

CNGB1 is specifically expressed in rod photoreceptors, which are the primarily affected cell type in *CNGB1*-RP and, thus, the target cells for gene supplementation therapy. The human rhodopsin promoter (*hRHO*) is one of the most established promoters for achieving a rod-specific expression and is already used for clinical gene therapy programs. However, because of the size of the full-length *hCNGB1* cDNA (>3.7 kb) and the additional space needed for minimally required regulatory (polyA) and viral (ITR) elements, incorporation of the previously characterized full-length (848 bp) *hRHO* promoter[26] would have resulted in an rAAV genome, which exceeds the packaging limit of AAVs (~4.7 kb). Therefore, we first aimed to design a shorter but still efficient and specific *hRHO* promoter version. In preliminary work, we truncated the

full length *hRHO* promoter aiming to conserve binding sites for important transcription factors such as Crx or Nrl.[27] A sufficiently short but still efficient and specific promoter version was a 194 bp sequence (hereafter termed *hRHO194*) corresponding to nucleotides 4816–5009 of NCBI Reference Sequence NG_009115.1 and comprising three known Crx and one Nrl binding site (Fig. 1A, for full sequence see Supplementary Fig. S1). We generated an AAV genome comprising a gene expression cassette for the full-length human *CNGB1* cDNA under control of this *hRHO194* promoter together with a short SV40 polyA sequence and AAV2-ITRs (Fig. 1A) and produced the AAV5 serotype vector rAAV5.hCNGB1, which results in solid expression of human CNGB1 (Fig. 1B).

In a dose-ranging study, rAAV5.hCNGB1 was injected at three different doses (low dose, 10^8; mid-dose, 10^9; high dose, 10^{10} total vg in 1 μL volume, respectively) into the subretinal space of 4-week-old *Cngb1*$^{-/-}$ mice. The contralateral eyes received 1 μL of vector diluent (BSS +0.014% Tween-20). After an in-life observation period of 9 months postinjection we dissected the retinae and performed immunohistochemical analysis to evaluate rAAV vector-derived human CNGB1 and endogenous mouse CNGA1 protein expression. Figure 1C–L illustrates typical immunosignals for CNGB1 (red) and CNGA1 (green) obtained in wild-type, sham-injected control and rAAV5.hCNGB1-treated *Cngb1*$^{-/-}$ mouse retina. The anti-CNGB1 antibody used detects both, the vector-derived human and the endogenous mouse CNGB1 protein. The endogenous mouse CNGB1 and CNGA1 proteins localize exclusively to the rod OS (Fig. 1C, D). Treatment with rAAV5.hCNGB1 resulted in a dose-dependent expression of human CNGB1 (red) in the photoreceptor layer (Fig. 1E, G, I), whereas there was no visible CNGB1 signal in the sham control *Cngb1*$^{-/-}$ retina (Fig. 1K). Of importance, as already shown for the species-matched gene supplementation therapy,[9,10] expression of human CNGB1 rescued the expression of the endogenous mouse CNGA1 protein (Fig. 1F, H, J), which in *Cngb1*$^{-/-}$ mice is degraded in the absence of the endogenous mouse CNGB1 protein.[5,10] Of note, although the rescued endogenous murine CNGA1 protein always localized exclusively to the OS layer, a substantial amount of vector-encoded human CNGB1 protein was found in the inner segments and throughout the photoreceptor layer (Fig. 1E, G, I). The 10^9 vg (mid-dose) dose of rAAV5.hCNGB1 also resulted in preservation of about eight rows of photoreceptors (Fig. 1G, H), whereas only one to two rows remained in the sham control *Cngb1*$^{-/-}$ retina (Fig. 1K, L).

These findings confirmed efficient and long-lasting (throughout the 9-month observation period) rAAV5.hCNGB1-driven transgene expression and efficient reactivation/rescue of endogenous CNGA1 expression, and suggested the mid-dose (10^9 vg) as the optimal dose.

rAAV5.hCNGB1 results in reactivation of rod CNG channels and gain of rod function

To confirm formation of functional chimeric (mouse alpha/human beta subunit) rod CNG channels, we utilized an indirect immunohistochemical readout based on the immunolocalization of the paraformaldehyde-fixed second messenger cGMP, which was shown to accumulate in *Cngb1*$^{-/-}$ rods owing to a missing Ca^{2+}-mediated negative feedback on the cGMP-producing rod guanylate cyclase.[10,25] As the natural ligand of CNG channels, cGMP binds to and activates the channels in the dark resulting in a mixed Na^+/Ca^{2+} inward current, which depolarizes the photoreceptor. In *Cngb1*$^{-/-}$ rods, the missing Ca^{2+} influx prevents deactivation of cGMP production leading to accumulation inside the photoreceptor cell. To test how the rAAV5.hCNGB1 treatment affects the levels of the cGMP, we performed immunolabeling with an anti-cGMP antibody (Fig. 2). The anti-cGMP antibody showed a clearly detectable cGMP signal in rod inner segment and OS in the untreated *Cngb1*$^{-/-}$ retina (the untreated part of a mid-dose-treated *Cngb1*$^{-/-}$ retina is given in Fig. 2C), indicating intracellular accumulation of cGMP, which in the wild type is normally efficiently degraded and nondetectable using these staining conditions (Fig. 2A). In the treated part of a mid-dose-treated *Cngb1*$^{-/-}$ retina, the cGMP signal was decreased (Fig. 2E), demonstrating a normalization of cGMP turnover, and thereby indirectly confirming a rAAV5.hCNGB1-dependent expression of a functional CNG channel in treated rods. Treatment at low dose (10^8 vg) or high dose (10^{10} vg) did not show a similar effect on the cGMP levels (Supplementary Fig. S2).

To analyze the rod-dependent retinal function in more detail, the study included multiple ERG measurements

Figure 1. rAAV5.hCNGB1 results in a dose-dependent, efficient, rod-specific transgene expression in the *Cngb1*$^{-/-}$ retina. **(A)** Cartoon illustrating the gene expression cassette of rAAV5.hCNGB1. The novel human rhodopsin promoter is shown in higher detail and important transcription factor binding sites are marked. **(B)** Representative overview image of a confocal scan through a treated *Cngb1*$^{-/-}$ mouse retina covering treated (within the subretinal bleb) and untreated (outside the subretinal bleb) parts. The treatment border is marked with a *dashed line*. **(C–L)** Representative confocal images showing expression of CNGB1 (*red*, the antibody detects mouse and human CNGB1) and CNGA1 protein (*green*) in retinal cross sections of wild type **(C, D)**, treated **(E–J)**, and sham-injected control *Cngb1*$^{-/-}$ mouse retinae **(K, L)** at 10 months of age (9 months postinjection). *Cngb1*$^{-/-}$ mice were injected at 4 weeks of age with rAAV5.hCNGB1 at low dose (10^8 vg; **E, F**), mid-dose (10^9 vg; **G, H**) or high dose (10^{10} vg; **I, J**). Dependent on the dose, varying amounts of hCNGB1 protein (*red*) were found in the OS, the IS, and the ONL of all treated *Cngb1*$^{-/-}$ mice. Endogenous CNGA1 (*green*) expression was rescued in a dose-dependent manner and the protein localized to the OS of the treated area. Cell nuclei were stained with DAPI (*blue*). The edges of the ONL are marked with *horizontal bars* **(C, E, G, I** and **K)**. GCL, ganglion cell layer; ONH, optic nerve head; OPL, outer plexiform layer. Scale bar in **(B)** marks 100 μm. Scale bar for **(C–L)** are shown in **(K)** and **(L)** and mark 25 μm. *Cngb1*, channel subunit beta 1; IS, inner segments; ONL, outer nuclear layer; OS, outer segments; vg, vector genomes. Color images are available online.

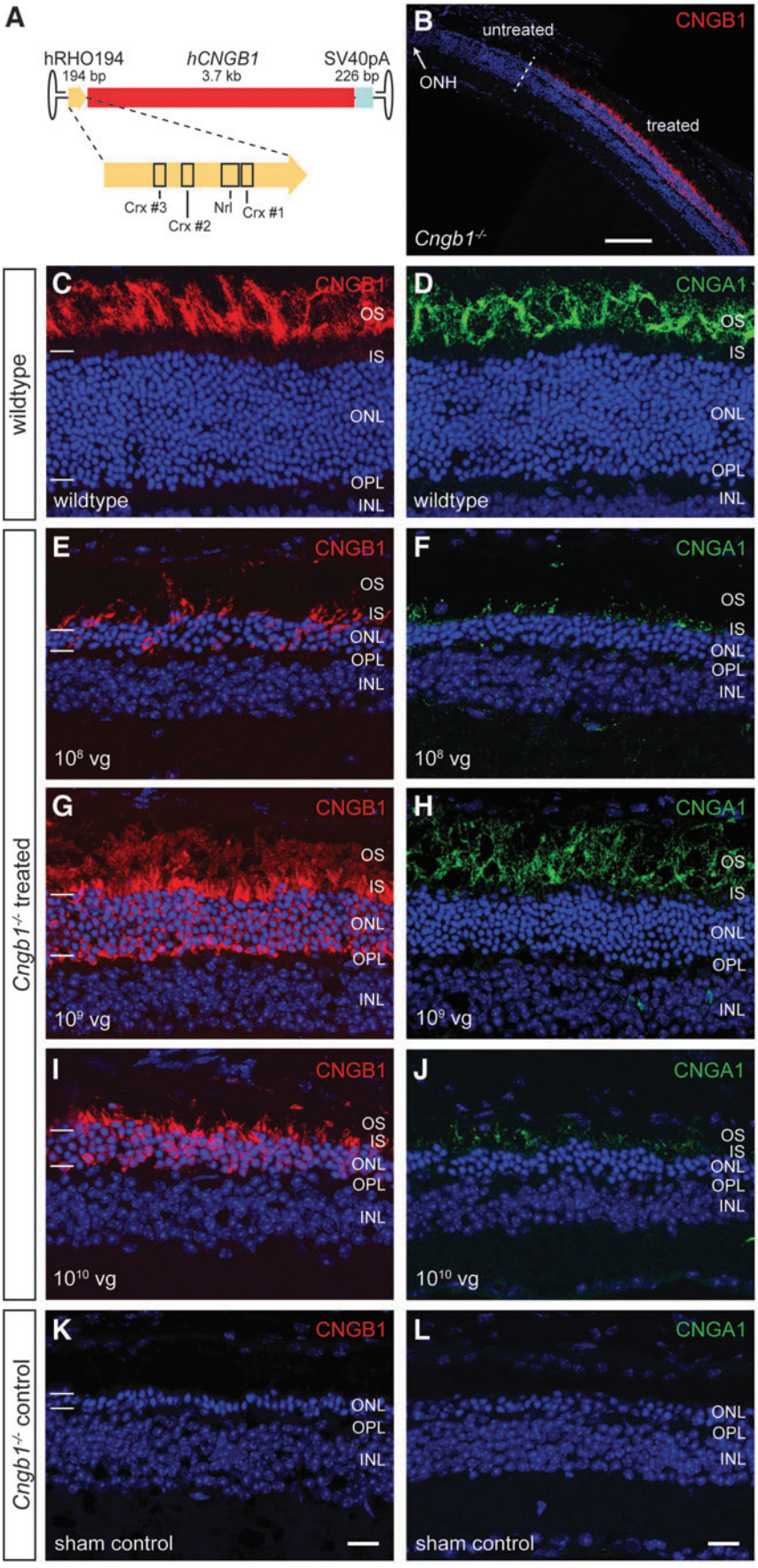
A
hRHO194
194 bp
hCNGB1
3.7 kb
SV40pA
226 bp
Crx #3
Crx #2
Nrl
Crx #1
B
CNGB1
untreated
ONH
treated
Cngb1-/-
wildtype
C
CNGB1
OS
IS
ONL
OPL
INL
wildtype
D
CNGA1
OS
IS
ONL
OPL
INL
wildtype
Cngb1-/- treated
E
CNGB1
OS
IS
ONL
OPL
INL
10^8 vg
F
CNGA1
OS
IS
ONL
OPL
INL
10^8 vg
G
CNGB1
OS
IS
ONL
OPL
INL
10^9 vg
H
CNGA1
OS
IS
ONL
OPL
INL
10^9 vg
I
CNGB1
OS
IS
ONL
OPL
INL
10^10 vg
J
CNGA1
OS
IS
ONL
OPL
INL
10^10 vg
Cngb1-/- control
K
CNGB1
ONL
OPL
INL
sham control
L
CNGA1
ONL
OPL
INL
sham control

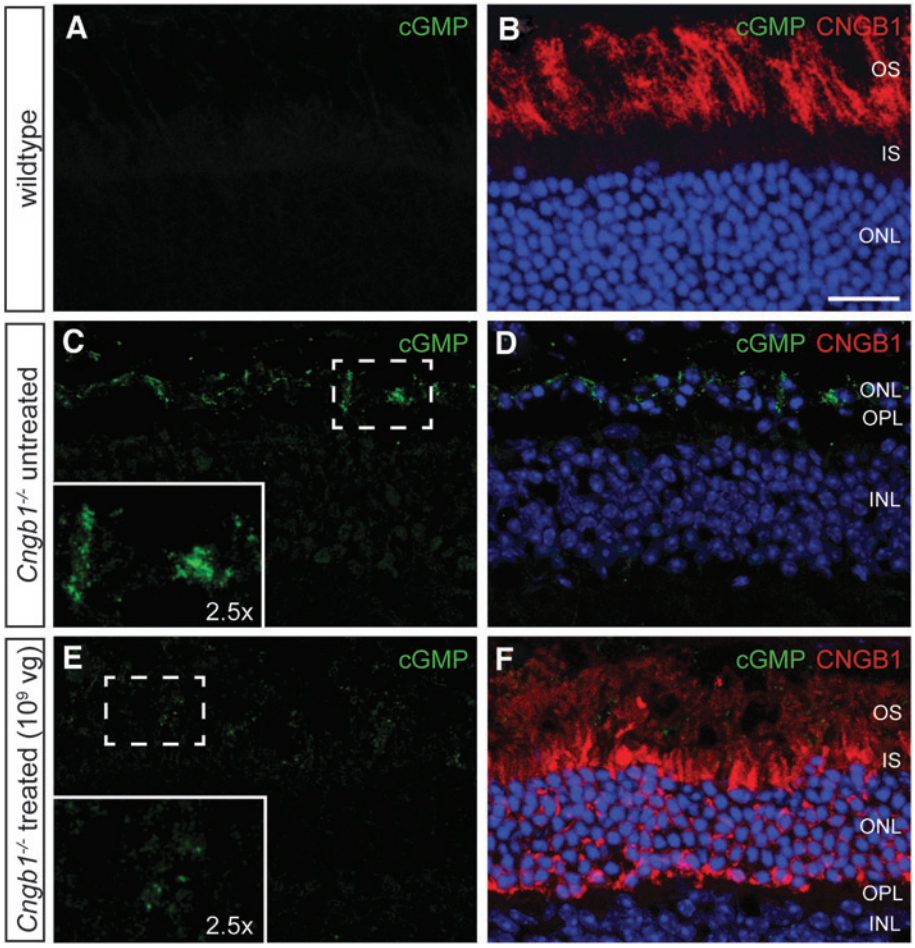

Figure 2. Normalization of cGMP levels suggests formation of functional chimeric rod CNG channels after treatment with rAAV5.hCNGB1. Representative confocal images of retinal cross sections of a wild-type mouse retina **(A, B)** and the untreated **(C, D)** and treated parts **(E, F)** of a mid-dose–treated (10^9 vg) *Cngb1*$^{-/-}$ mouse at 10 months of age. The sections were immunolabeled with anti-cGMP (*green*) and anti-CNGB1 (*red*). An accumulation of cGMP was observed in the OS of the untreated part of the *Cngb1*$^{-/-}$ retina, whereas cGMP accumulation was reduced in the treated part. Cell nuclei in **(B, D,** and **F)** were stained with DAPI (*blue*). Scale bar marks 25 μm. cGMP, cyclic guanosine monophosphate; CNG channel, cyclic nucleotide-gated channel. Color images are available online.

during the in-life phase. ERG was performed on dark-adapted animals using a series of light stimuli at increasing luminance, including the ISCEV rod-specific standard luminance of 0.01 cd s m^{-2}. Although signals obtained in *Cngb1*$^{-/-}$ wild-type mice showed clear positive deflections (b wave) of the ERG amplitude (Supplementary Fig. S2A–C, gray lines), signals obtained in untreated (sham-injected) *Cngb1*$^{-/-}$ mice were strongly reduced throughout the range of light stimuli (Fig. 3A and Supplementary Fig. S3A, black lines). At the rod-specific luminance (0.01 cd s m^{-2}), a response could not be detected. However, mid-dose treatment of rAAV5.hCNGB1 (Fig. 3A, B and Supplementary Fig. S3A, B, middle graphs, magenta lines; Supplementary Fig. S4C, D) demonstrated a clear increase of b-wave amplitudes compared with the sham-injected contralateral eye especially at rod-specific light stimuli ranges of 0.01 and 0.03 cd s m^{-2}. In addition, a slight recovery of a-wave signals could be seen with the mid-dose treatment starting from 0.1 cd s m^{-2} upward. Furthermore, ERG measurements of low-dose-treated *Cngb1*$^{-/-}$ mice (Fig. 3A, B and Supplementary Fig. S3A, B, left graphs, green lines; Supplementary Fig. S4A, B) also showed increased responses to different light stimuli, whereas high-dose treatment (Fig. 3A, B and Supplementary Fig. S3A, B, right graphs, orange lines; Supplementary Fig. S4E, F) failed to show obvious improvements. Despite a general decline of amplitudes, 9 months follow-up data (Fig. 3C and Supplementary Fig. S3C, middle graph, magenta line; Supplementary Fig. S4C, D) showed a sustained functional benefit with twofold higher b-wave amplitudes for mid-dose treatment compared with the control, confirming a long-term beneficial effect of rAAV5.hCNGB1 treatment on rod function until an advanced stage of the disease. Although less prominent, a long-term beneficial effect was also seen in the low-dose treatment group (Fig. 3C and Supplementary Fig. S3C, left graph, green line; Supplementary Fig. S4A, B), whereas no differences in b-wave amplitudes were

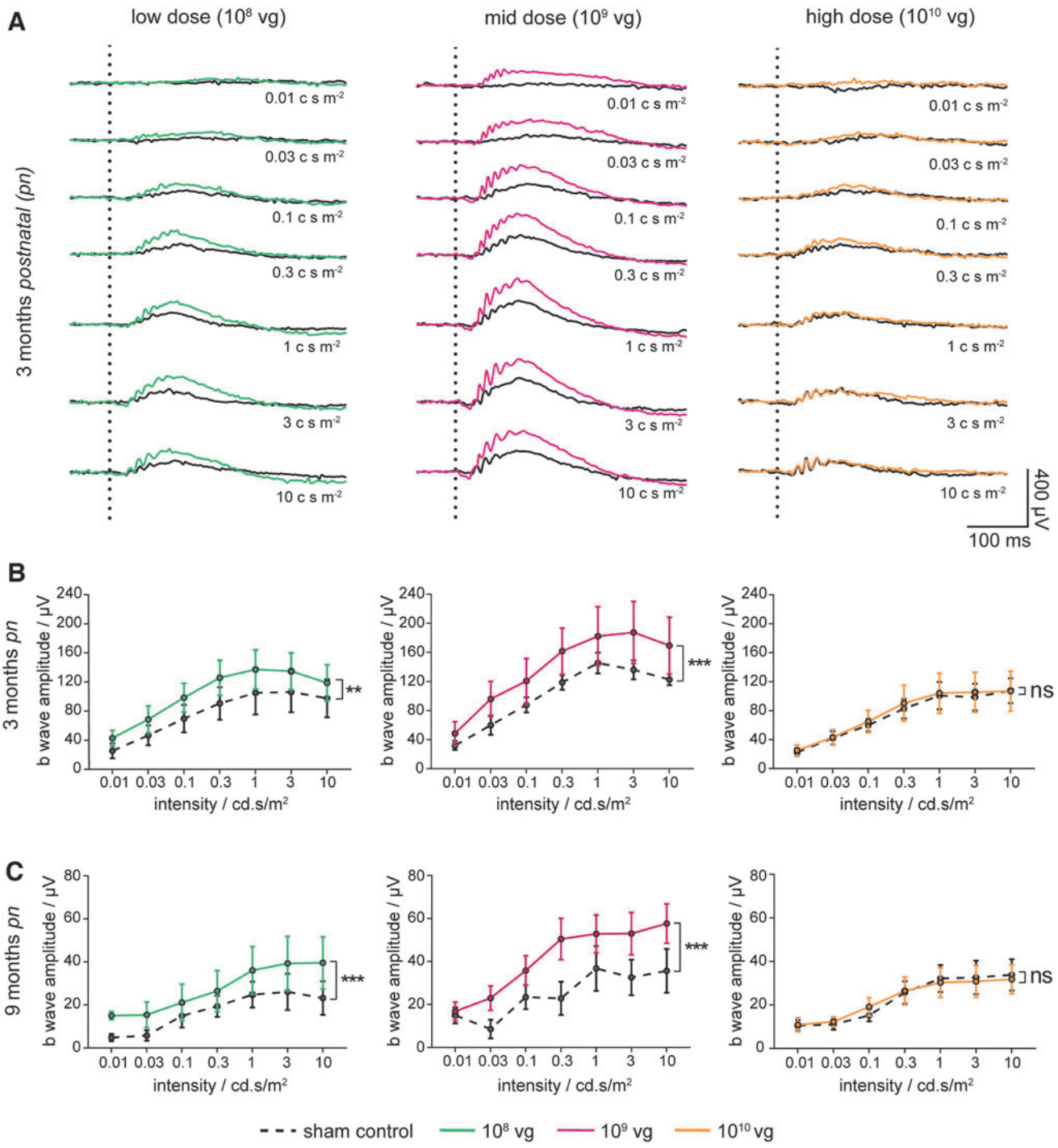

Figure 3. rAAV5.hCNGB1 leads to a dose-dependent gain of rod-driven ERG amplitudes in treated *Cngb1*$^{-/-}$ mice. **(A)** Overlays of representative ERG signals of 3-month-old–treated *Cngb1*$^{-/-}$ mice injected with different doses (low dose 10^8 vg; mid-dose 10^9 vg; high dose 10^{10} vg) of rAAV5.hCNGB1 at 4 weeks. Vertical *dotted lines* mark the time point of light stimulation. Respective sham-injected contralateral eyes served as controls showing almost no (rod-mediated) response at low light intensities (0.01 and 0.03 cd s m^{-2}). Mid-dose treatment (*magenta lines*) showed highest gain in photoreceptor function compared with the respective sham-injected control (*black lines*). In this group the b-wave amplitude (positive deflection) obtained under low light intensities was clearly higher in the treated than in the sham-injected control eye. A treatment effect was also evident at higher luminances. In contrast, only a small increase was seen in ERG signals after treatment at low dose (*green lines*) and no obvious differences observed after high-dose (*orange line*) treatment compared with sham-injected control eyes. **(B, C)** Quantification of b-wave amplitudes of treated and sham injected *Cngb1*$^{-/-}$ eyes at 3 and 9 months of age shows a dose-dependent beneficial effect on retinal function. Mid-dose and to a lesser extent low-dose treatment resulted in significantly increased b-wave amplitudes, whereas treatment at high dose did not cause any difference on the ERG b-wave. Although overall amplitudes declined over time, a significant gain of ERG function was seen at 9 months of age suggesting a long-term benefit of rAAV5.hCNGB1 treatment. For 3 months *pn*: low dose $n=7$, mid-dose $n=6$, high dose $n=6$; for 9 months *pn*: low dose $n=7$, mid-dose $n=7$, high dose $n=10$. Values are given as mean ± SEM (unpaired two-way ANOVA with Sidak's *post hoc* test; $^{**}p \leq 0.01$; $^{***}p \leq 0.001$; ns, not significant). ANOVA, analysis of variance; ERG, electroretinography; pn, postnatal; SEM, standard error of the mean. Color images are available online.

seen between the high-dose treatment and the control group (Fig. 3C and Supplementary Fig. S3C, right graph, orange line; Supplementary Fig. S4E, F). Thus, assessment of rod-driven retinal function with ERG confirmed long-term restoration of photoreceptor function after subretinal gene therapy with rAAV5.hCNGB1 and established the mid-dose (10^9 vg) as optimal dose.

rAAV5.hCNGB1 treatment leads to improved vision-guided behavior

Previous studies with species-matched gene supplementation therapy[9,10] provided evidence for treatment-dependent improvements of vision. To confirm that the chimeric mouse/human rod CNG channel can also have beneficial effects on vision, we assessed vision-guided behavior in treated *Cngb1*$^{-/-}$ mice. In particular, we observed spatial navigation in a visual water maze task at 9 months scoring the ability and measuring the latency of mid-dose–treated and untreated *Cngb1*$^{-/-}$ mice and wild-type control mice to locate a visible swimming platform (Fig. 4). Initial testing was performed for two consecutive days under light conditions that require rod function (dark; see details in Materials and Methods section). Representative swimming routes of the three test groups under these dark conditions are given in Fig. 4A. When placed into the water-filled tank, wild-type mice instantly localized and navigated to the visible floating platform and showed a 100% success rate on the second testing day (Fig. 4B, C and Supplementary Fig. S5, gray line). In contrast, untreated *Cngb1*$^{-/-}$ mice often struggled to locate the visible platform and showed overall six times longer latencies than wild-type mice (Fig. 4B, C and Supplementary Fig. S5, black line). Vision-guided behavior was not assessed in the high-dose treated group given the lack of improvement in the ERG. Low-dose–treated *Cngb1*$^{-/-}$ mice did not show significant improvement in navigating in the dark (Supplementary Fig. S5, green line). However, confirming the rAAV5.hCNGB1-mediated gain in vision, mid-dose–treated *Cngb1*$^{-/-}$ mice performed with higher fidelity (close to 90% on day 2) and reached the platform after an averaged latency of ~45 s on day 1 and further improved by day 2 to a mean latency time of ~30 s (Fig, 4B, C and Supplementary Fig. S5, magenta line). Thus, mid-dose rAAV5.hCNGB1-treated *Cngb1*$^{-/-}$ mice

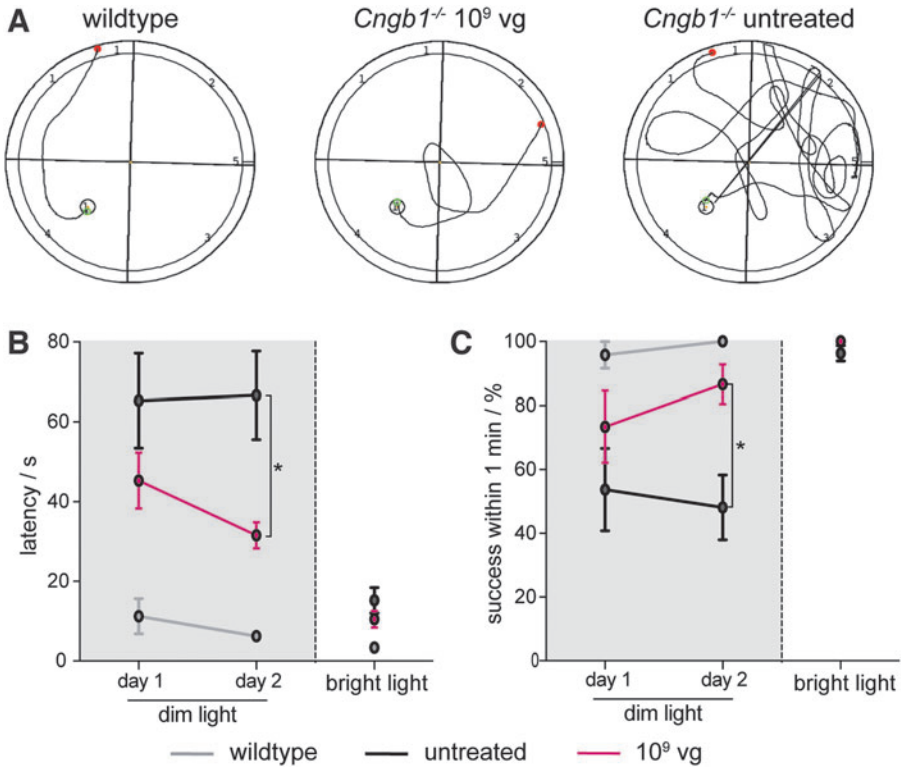

Figure 4. rAAV5.hCNGB1 results in improved spatial navigation of treated *Cngb1*$^{-/-}$ mice under dim light conditions. **(A)** Representative swimming tracks of 9-month-old wild-type ($n=4$), untreated ($n=9$) and mid-dose–treated (treated at 4 weeks with 10^9 vg of rAAV5.hCNGB1; $n=5$) *Cngb1*$^{-/-}$ mice in a visual water maze task under dim light conditions. **(B)** Quantification of latency time until a visible swimming platform was reached during two dim light and one bright light testing days. In contrast to untreated *Cngb1*$^{-/-}$ mice, those treated with rAAV5.hCNGB1 could improve their performance from days 1 to 2 and needed a shorter time to find the platform on the second test day. **(C)** Quantification of the success score to locate the swimming visible platform within 1 min (percentage of total runs). Untreated *Cngb1*$^{-/-}$ mice had a chance success rate of ~50% on both dim light test days. Again, treated *Cngb1*$^{-/-}$ mice could improve their performance on reaching a success rate of >80% on day 2. **(B, C)** Mice from all test groups performed well on the third test day under bright light confirming sufficient remaining cone-mediated vision functionality in the untreated *Cngb1*$^{-/-}$ mice. Values are given as mean ± SEM (unpaired two-way ANOVA with Sidak's *post hoc* test; $*p \leq 0.05$). Color images are available online.

navigated significantly faster in this task than the untreated control group. On the final testing day, the mice were tested under bright light conditions to confirm their principal ability to solve the task and exclude confounding factors, such as surgery-related collateral retinal damage. As given in Fig. 4B, C, mice from all test groups were able to find the platform with a latency of <20 s, proving that cone-mediated visual function was still sufficiently preserved to navigate under bright light conditions. Taken together, rAAV5.hCNGB1-treated *Cngb1*$^{-/-}$ mice showed a gain in spatial navigation at least until 9 months of age supporting the view that treated mice were able to properly process recovered photoreceptor function.

rAAV5.hCNGB1 treatment preserves photoreceptor layer thickness in treated *Cngb1*$^{-/-}$ mice

CNGB1-RP is characterized by degeneration and loss of photoreceptors,[2,3,9] which is also observed in the animal models and can be monitored over time using SD-OCT.[9] In *Cngb1*$^{-/-}$ mice shortening of rod OS is already evident shortly after eye opening at postnatal day 15.[5] With progression of rod photoreceptor degeneration, the thickness of outer nuclear layer (ONL) continuously decreases, resulting in an almost absent ONL at the age of 10 months.[9] To assess the effect of rAAV5.hCNGB1 treatment on the progression of photoreceptor degeneration in *Cngb1*$^{-/-}$ mice, we performed *in vivo* SD-OCT measurements at 3, 5, and 9 months of age during the in-life phase of the dose-ranging study. A representative SD-OCT scan through the retina of a 9-month-old (8 months postinjection) mid-dose–treated *Cngb1*$^{-/-}$ mouse spanning the treated (previous subretinal bleb area) and untreated part of the retina is given in Fig. 5A. The treatment resulted in a clear preservation of both ONL and photoreceptor OS layer thickness (Fig. 5B), whereas both layers were severely thinned and hardly discernable in the untreated area (Fig. 5C). Nonphotoreceptor retinal structures, such as the inner nuclear layer (INL), ganglion cell layer (GCL) or the retinal pigment epithelium were not visibly affected and treatment with rAAV5.hCNGB1 did not cause any obvious morphological alterations in these structures. Quantification of SD-OCT scans from sham-injected contralateral *Cngb1*$^{-/-}$ mice eyes (dashed lines in Fig. 5D–F) confirmed a steady decrease of photoreceptor layer thickness over time, whereas for the wild-type control it remained at $\sim 110\,\mu$m (gray lines in Fig. 5D–F). Although rAAV5.hCNGB1 treatment could not arrest the progression of photoreceptor layer thinning, it resulted in a clear deceleration as evident from the significantly preserved photoreceptor layer thicknesses in treated groups (Fig. 5D–F and Supplementary Fig. S6). Morphological preservation was best at mid-dose (10^9 vg), but also observed in the low-dose (10^8 vg) group. Despite the lack of functional improvements in the ERG measurements, a small but significant preservation effect could still be seen by SD-OCT in the high-dose (10^{10} vg) group. Thus, in addition to the functional gain, gene supplementation therapy with rAAV5.hCNGB1 also led to a long-lasting, dose-dependent preservation of photoreceptor morphology in *Cngb1*$^{-/-}$ mice.

rAAV5.hCNGB1 treatment prolongs cone photoreceptor survival and reduces Müller cell gliosis in treated *Cngb1*$^{-/-}$ mice

Secondary to rods, cone photoreceptors also degenerate despite not being directly affected by the *Cngb1* mutation. Given the importance of cone photoreceptor-mediated daylight vision, the long-term aim of gene supplementation therapy is to prevent the secondary loss of cones in *CNGB1*-RP patients. In *Cngb1*$^{-/-}$ mice, cone degeneration usually starts at $\sim$6 months of age.[5,9] As cones make up only $\sim$3% of all photoreceptors in the mouse retina,[28,29] OCT measurement cannot visualize a potential rescue effect on cone structure and/or cell number. Therefore, we analyzed the effect of the rAAV5.hCNGB1 treatment by immunohistochemistry using the specific marker cone arrestin, which in the wild type labels the entire cone cell including, OS and inner segment, cell body, axon, and synapse (Fig. 6A, A′). In the untreated area of a mid-dose–treated (10^9 vg; rAAV5.hCNGB1) *Cngb1*$^{-/-}$ mouse retina the cone arrestin signal was still present; however, the labeled remaining cone structures did not show the characteristic normal cone photoreceptor morphology (Fig. 6B, B′). OS and inner segment were completely degenerated and merely the spherical cell bodies and remnants of synapses were still visible. In contrast, the treated part of the same retina showed intact cones with the characteristic wild-type–like morphology (Fig. 6C, C′). Cone cell body and synapse was still properly positioned and the radial cone cells spanned the entire remaining ONL. Apparently, the cone photoreceptor axons seemed to have adjusted their length to fit into the thinner ONL (Fig. 6C, C′).

The Müller glia cells are another cell type of the *Cngb1*$^{-/-}$ retina, which shows changes secondary to the photoreceptor degeneration. In particular, it was shown that in response to rod degeneration Müller glia cells upregulate glial fibrillary acidic protein (GFAP) expression.[5] Reduction of GFAP levels was already demonstrated as a result of murine *Cngb1* gene supplementation.[10] To prove whether supplementation of human *CNGB1* can also reduce GFAP levels, cross-sections of mid-dose–treated (10^9 vg) *Cngb1*$^{-/-}$ retinas were immunolabeled for GFAP (Fig. 6D–F). In the wild type, GFAP only labels astrocytes and Müller cell end feet at the inner limiting membrane underneath the GCL (Fig. 6D). In contrast, strongly GFAP-immunopositive fibers can be observed in the untreated part of a treated *Cngb1*$^{-/-}$ retina (Fig. 6E) indicative of a reactive Müller cell gliosis.[30] Upon mid-dose treatment, a strong reduction of Müller cell gliosis was

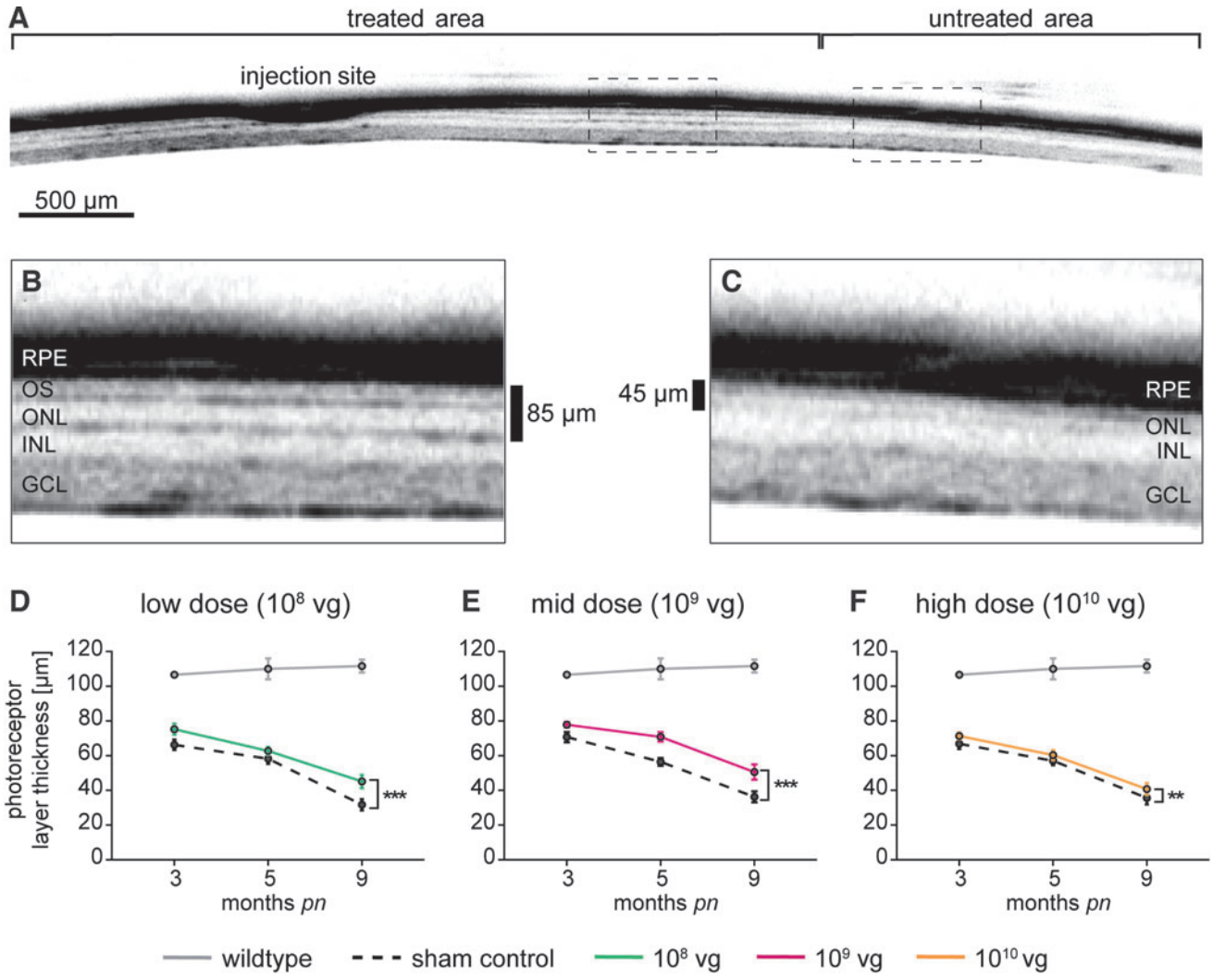

Figure 5. rAAV5.hCNGB1 gene therapy preserves photoreceptor layer thickness. **(A–C)** Representative SD-OCT images of a mid-dose–treated *Cngb1*$^{-/-}$ retina (10^9 vg; rAAV5.hCNGB1) at 9 months of age demonstrating preservation of photoreceptor layer thickness in the treated **(B)** compared with the untreated **(C)** area. In the untreated area only a single thin ONL remained. In contrast, the treated part shows characteristic multiple laminae for OS and ONL separated by a darker band representing the IS. **(D–F)** Quantification of photoreceptor layer thickness (μm) in 3-, 5-, and 9-month-old *Cngb1*$^{-/-}$ eyes after treatment with 10^8 vg (**D**; low dose), 10^9 vg (**E**; mid-dose) and 10^{10} vg of rAAV5.hCNGB1 (**F**; high dose) at 4 weeks compared with their respective sham-injected contralateral eyes and wild type. Significant preservation of photoreceptors structure was seen in all dose groups, the treatment effect was strongest at mid-dose. Wild type $n=3$; low dose $n=7$; mid-dose $n=7$; high dose $n=9$, owing to technical reasons only $n=8$ for 3 months. Values are given as mean ± SEM (two-way ANOVA paired with Sidak's *post hoc* test; $^{**}p \leq 0.01$, $^{***}p \leq 0.001$). SD-OCT, spectral-domain optical coherence tomography. Color images are available online.

observed in the treated part of the same *Cngb1*$^{-/-}$ retina (Fig. 6F). In contrast, low- and high-dose treatment did not reduce Müller cell gliosis (Supplementary Fig. S7). In summary, these data demonstrate that treatment with rAAV5.hCNGB1 preserves cone morphology, providing the basis for maintained daylight vision and reduces Müller cell gliosis suggesting a positive effect of the treatment on degeneration-induced retinal stress.

DISCUSSION

RP is the most common inherited retinal disorder affecting >2 million people worldwide. *CNGB1* in one of probably >100 different, mostly rod photoreceptor-expressed genes linked to RP.[2,31] Despite encouraging preclinical proof-of-concept studies with rAAV-mediated species-matched gene supplementation in mice and dogs,[9,10] there is currently no treatment available. In this study, we developed rAAV5.hCNGB1, a novel translatable rAAV vector for specific gene supplementation/augmentation of human *CNGB1* in rods and show that a one-time subretinal treatment results in a dose-dependent functional benefit and long-term rescue of the RP phenotype in the well-characterized *Cngb1*$^{-/-}$ mouse model of RP type 45 (RP45).

CNGB1 encodes the B1 (or beta 1) subunit of the rod CNG channel, which together with the A1 (or alpha 1) subunit encoded by *CNGA1* forms the native cGMP-gated cation channel found in the rod OS plasma membrane.[4]

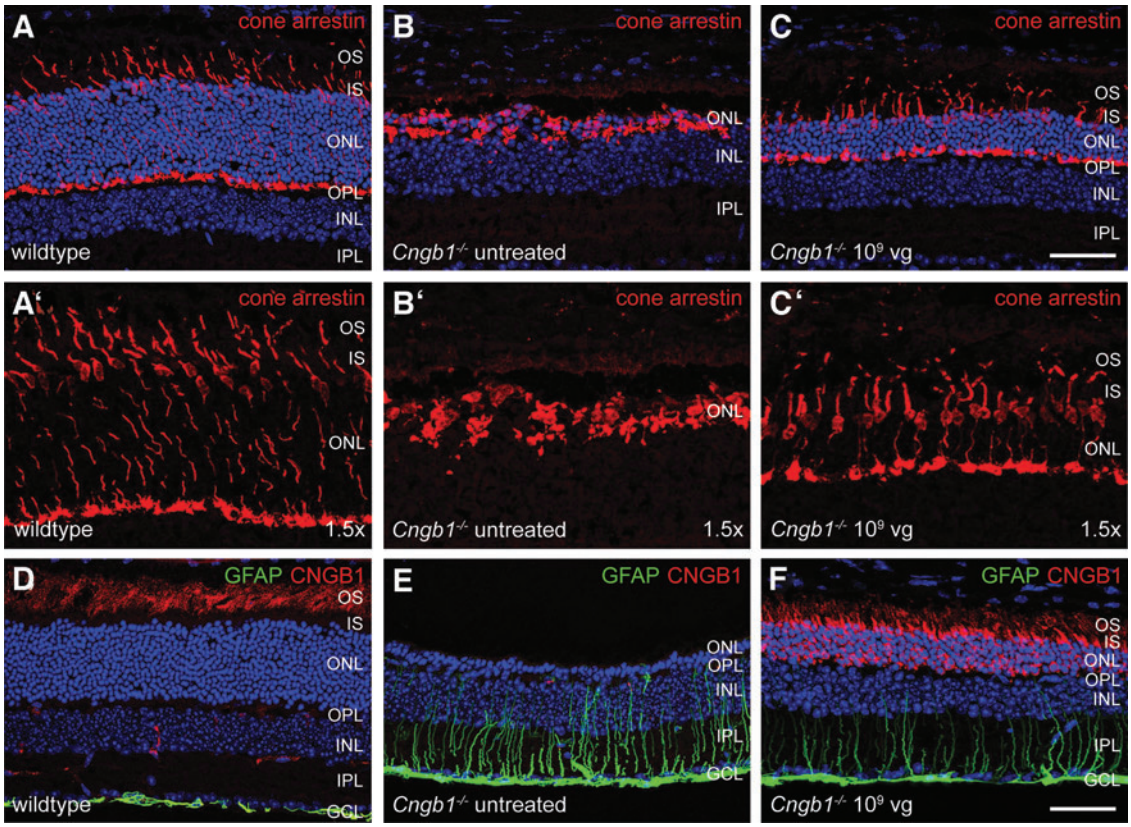

Figure 6. rAAV5.hCNGB1 treatment prevents secondary degeneration of cone photoreceptors and reduces Müller cell gliosis. (**A–C** and 1.5×magnifications in **A′–C′**) Representative confocal images from retinal cross sections of wild type **(A, A′)**, untreated part **(B, B′)**, and treated part **(C, C′)** of a mid-dose–treated (10^9 vg, rAAV5.hCNGB1) *Cngb1*$^{-/-}$ retina at 10 months of age (9 months after treatment). Although the cone arrestin marker (*red*) stained only spherical (presumably) cone cell bodies and cell residues in the untreated part, it revealed a preserved wild-type–like morphology of cones with all characteristic compartments including OS and IS an axon transecting the entire (still remaining) ONL and a cone pedicle at the OPL in the treated part. (**D–F**) Representative confocal images from retinal cross sections of wild type **(D)**, untreated part **(E)**, and treated part **(F)** of a mid-dose–treated (10^9 vg, rAAV5.hCNGB1) *Cngb1*$^{-/-}$ retina at 10 months of age immunostained for the Müller glia marker GFAP and for CNGB1 (the antibody detects mouse and human CNGB1). Mid-dose treatment caused a decrease of GFAP expression **(F)**, which is strongly upregulated in the untreated part **(E)** owing to retinal stress induced Müller cell gliosis. Scale bars mark 50 μm. GFAP, glial fibrillary acidic protein; IPL, inner plexiform layer. Color images are available online.

Despite being only a modulatory subunit, CNGB1 is indispensable for expression, intracellular transport, proper localization, and functionality of the rod CNG channel.[5–7,32,33] This is exemplified by the finding that the CNGA1 protein is not sufficiently transported to the rod OS in the absence of CNGB1, and thus degraded and barely present in rod OS of mouse and dog models of CNGB1 deficiency.[5–7] This secondary loss of CNGA1 protein could be rescued after ''species-matched'' rAAV vector-mediated expression of murine *Cngb1* in *Cngb1*$^{-/-}$ mice[10] or canine *Cngb1* in *Cngb1*-deficient dogs.[9] In this study, we showed that human CNGB1, when expressed after treatment of *Cngb1*$^{-/-}$ mice with rAAV5.hCNGB1, can rescue the endogenous mouse CNGA1 protein from degradation and leads to efficient and proper localization of this CNG subunit in mouse rod OS. Our data suggest that these chimeric mouse CNGA1/human CNGB1 heterotetrameric ion channel complexes are not only formed *in vivo*, but are also functional. This is supported by our finding that (1) rAAV5.hCNGB1 treatment normalized the aberrantly high levels of the second messenger cGMP in *Cngb1*$^{-/-}$ rods, which accumulates in the absence of CNG channel function owing to a missing Ca^{2+}-dependent and guanylate cyclase activator-mediated negative feedback on the cGMP-producing retinal guanylate-cyclase[34,35] and (2) rAAV5.hCNGB1 gene therapy led to improvements of retinal function and vision as detected by ERG and vision-guided behavior, respectively. Of note, the rescued endogenous CNGA1 protein exclusively localized to rod OS as expected from the native rod CNG channel.[5] Depending on the dose, only a fraction of hCNGB1 showed the same rod OS localization, whereas substantial amounts of the human CNGB1 protein was found in the inner segment and the synaptic compartments. It is tempting to speculate that formation of chimeric human CNGB1 and mouse CNGA1 channel complexes is not as efficient as in the species-matched situation in which most of the rAAV vector-derived CNGB1 protein showed normal rod OS localization.[9,10] The reason for this is not known, but might be related to the only ~68%. cross-species identity

between the mouse and human CNGB1 protein. Given that the mislocalized hCNGB1 protein did not colocalize with CNGA1 and homomeric CNGB1-only complexes do not support an ion channel function,[36,37] we conclude that the functional benefits seen in our study could only result from the rod OS-localized fraction of hCNGB1. We cannot exclude toxic effects of too high levels of aberrantly localized hCNGB1 protein, which might be the reason why only a slight structural, but no functional preservation effect could be observed in the high-dose group. However, given that (1) even the high dose did not result in deleterious effects (*e.g.*, acceleration of the degeneration or loss of cone function), (2) no negative effects were seen in the mid- or low-dose groups and (3) no dose-dependent toxicity was reported from the studies with species-matched rAAV vectors, *CNGB1* gene supplementation therapy can be considered a valid approach for the treatment of *CNGB1*-RP. The results merely raise questions whether knockout mouse models are the optimal disease models for testing potency of translatable (human-specific) gene therapies.

Nevertheless, our study clearly showed that rAAV5.hCNGB1 treatment results in a dose-dependent expression of hCNGB1 and formation of a functional chimeric rod CNG channel in *Cngb1*$^{-/-}$ mouse rod photoreceptor OS. This reconstitution of a rod CNG channel leads to a gain of rod photoreceptor function and improvement of vision-guided behavior under dim-light conditions. Of importance, this functional restoration goes along with a clear preservation of rod photoreceptors and prevention of the otherwise inevitable secondary degeneration of cone photoreceptors. In addition, treatment with rAAV5.hCNGB1 also reduced Müller cell gliosis, which is commonly observed in retinal degeneration.

CONCLUSION

In this preclinical study, we demonstrate cross-species efficacy of the novel vector rAAV5.hCNGB1 designed as a gene therapy for the treatment of *CNGB1*-RP patients. rAAV5.hCNGB1 showed a dose-dependent and cell type-specific transgene expression, which led to a gain of rod function, improvement of rod-mediated vision concurred by a deceleration of primary retinal degeneration and prevention of secondary cone photoreceptor degeneration. Thus, rAAV5.hCNGB1 appears to be a suitable candidate for further translational studies in large animal models and future clinical application.

AUTHORS' CONTRIBUTIONS

S.M. conceptualization; S.M., L.Z., and J.E.W. writing; J.E.W., L.Z. performed experiments; S.M. designed the rAAV vector; C.R.O'R. and A.F. produced rAAVs; M.B. and S.M. generated the mouse model; J.E.W., L.Z., S.M., M.J.G., and S.M.P.-J. analyzed data; S.M., S.M.P.-J., and M.B acquired funding.

ACKNOWLEDGMENTS

The authors thank Johanna Koch and Kerstin Skokann for excellent technical help, Hermann Ammer (LMU Munich) for help with the design and generation of anti-CNGA1 and anti-CNGB1 antibodies and Wolfgang Baehr (University of Utah) for the gift of anti-cone arrestin antibody.

AUTHOR DISCLOSURE

S.M. and M.B. are inventors on the patent application WO2018172961A1 ''Gene therapy for the treatment of cngb1-linked retinitis pigmentosa'' and co-founders of the gene therapy company ViGeneron GmbH. C.R.O'R. and A.F. are employees of Sanofi Corporation. All other authors declare no competing interests.

FUNDING INFORMATION

This work was supported by the NEI of the National Institutes of Health under award number R24EY027285 (to S.M. and S.M.P.-J.) and by Sanofi (to S.M. and M.B.).

SUPPLEMENTARY MATERIAL

Supplementary Data
Supplementary Figure S1
Supplementary Figure S2
Supplementary Figure S3
Supplementary Figure S4
Supplementary Figure S5
Supplementary Figure S6
Supplementary Figure S7

REFERENCES

1. Hartong DT, Berson EL, Dryja TP. Retinitis pigmentosa. Lancet 2006;368:1795–1809.
2. Nassisi M, Smirnov V, Hernandez CS, et al. CNGB1-related rod-cone dystrophy: a mutation review and update. Hum Mutat 2021;42:641–666.
3. Hull S, Attanasio M, Arno G, et al. Clinical characterization of CNGB1-related autosomal recessive retinitis pigmentosa. JAMA Ophthalmol 2017;135:137–144.
4. Michalakis S, Becirovic E, Biel M. Retinal cyclic nucleotide-gated channels: from pathophysiology to therapy. Int J Mol Sci 2018;19:749.
5. Hüttl S, Michalakis S, Seeliger M, et al. Impaired channel targeting and retinal degeneration in mice lacking the cyclic nucleotide-gated channel subunit CNGB1. J Neurosci 2005;25:130–138.
6. Zhang Y, Molday LL, Molday RS, et al. Knockout of GARPs and the beta-subunit of the rod cGMP-gated channel disrupts disk morphogenesis and rod outer segment structural integrity. J Cell Sci 2009;122:1192–1200.

7. Winkler PA, Ekenstedt KJ, Occelli LM, et al. A large animal model for CNGB1 autosomal recessive retinitis pigmentosa. PLoS One 2013;8: e72229.

8. Pearring JN, Martinez-Marquez J, Willer JR, et al. The GARP domain of the rod CNG channel's beta1-subunit contains distinct sites for outer segment targeting and connecting to the photoreceptor disk rim. J Neurosci 2021;41:3094–3104.

9. Petersen-Jones SM, Occelli LM, Winkler PA, et al. Patients and animal models of CNGbeta1-deficient retinitis pigmentosa support gene augmentation approach. J Clin Invest 2018;128:190–206.

10. Koch S, Sothilingam V, Garcia Garrido M, et al. Gene therapy restores vision and delays degeneration in the CNGB1(-/-) mouse model of retinitis pigmentosa. Hum Mol Genet 2012;21:4486–4496.

11. Mattapallil MJ, Wawrousek EF, Chan CC, et al. The Rd8 mutation of the Crb1 gene is present in vendor lines of C57BL/6N mice and embryonic stem cells, and confounds ocular induced mutant phenotypes. Invest Ophthalmol Vis Sci 2012;53: 2921–2927.

12. Becirovic E, Nakova K, Hammelmann V, et al. The retinitis pigmentosa mutation c.3444 + 1G>A in CNGB1 results in skipping of exon 32. PLoS One 2010;5:e8969.

13. Samulski RJ, Chang LS, Shenk T. A recombinant plasmid from which an infectious adeno-associated virus genome can be excised in vitro and its use to study viral replication. J Virol 1987; 61:3096–3101.

14. Schön C, Sothilingam V, Mühlfriedel R, et al. Gene therapy successfully delays degeneration in a mouse model of PDE6A-linked retinitis pigmentosa (RP43). Hum Gene Ther 2017;28:1180–1188.

15. Schambach A, Galla M, Maetzig T, et al. Improving transcriptional termination of self-inactivating gamma-retroviral and lentiviral vectors. Mol Ther 2007;15:1167–1173.

16. Martin J, Frederick A, Luo Y, et al. Generation and characterization of adeno-associated virus producer cell lines for research and preclinical vector production. Hum Gene Ther Methods 2013;24:253–269.

17. Qu G, Bahr-Davidson J, Prado J, et al. Separation of adeno-associated virus type 2 empty particles from genome containing vectors by anion-exchange column chromatography. J Virol Methods 2007;140:183–192.

18. Nass SA, Mattingly MA, Woodcock DA, et al. Universal method for the purification of recombinant AAV vectors of differing serotypes. Mol Ther Methods Clin Dev 2018;9:33–46.

19. Mühlfriedel R, Michalakis S, Garrido MG, et al. Optimized subretinal injection technique for gene therapy approaches. Methods Mol Biol 2019; 1834:405–412.

20. Schön C, Asteriti S, Koch S, et al. Loss of HCN1 enhances disease progression in mouse models of CNG channel-linked retinitis pigmentosa and achromatopsia. Hum Mol Genet 2016;25:1165–1175.

21. Marmor MF, Fishman GA. At last. A standard electroretinography protocol. Arch Ophthalmol 1989;107:813–814.

22. Michalakis S, Geiger H, Haverkamp S, et al. Impaired opsin targeting and cone photoreceptor migration in the retina of mice lacking the cyclic nucleotide-gated channel CNGA3. Invest Ophthalmol Vis Sci 2005;46:1516–1524.

23. Michalakis S, Mühlfriedel R, Tanimoto N, et al. Restoration of cone vision in the CNGA3-/- mouse model of congenital complete lack of cone photoreceptor function. Mol Ther 2010;18:2057–2063.

24. Zhang T, Baehr W, Fu Y. Chemical chaperone TUDCA preserves cone photoreceptors in a mouse model of Leber congenital amaurosis. Invest Ophthalmol Vis Sci 2012;53:3349–3356.

25. Tanaka J, Markerink-van Ittersum M, Steinbusch HW, et al. Nitric oxide-mediated cGMP synthesis in oligodendrocytes in the developing rat brain. Glia 1997;19:286–297.

26. Allocca M, Mussolino C, Garcia-Hoyos M, et al. Novel adeno-associated virus serotypes efficiently transduce murine photoreceptors. J Virol 2007;81: 11372–11380.

27. Lee J, Myers CA, Williams N, et al. Quantitative fine-tuning of photoreceptor cis-regulatory elements through affinity modulation of transcription factor binding sites. Gene Ther 2010;17:1390–1399.

28. Jeon CJ, Strettoi E, Masland RH. The major cell populations of the mouse retina. J Neurosci 1998; 18:8936–8946.

29. Ortin-Martinez A, Nadal-Nicolas FM, Jimenez-Lopez M, et al. Number and distribution of mouse retinal cone photoreceptors: differences between an albino (Swiss) and a pigmented (C57/BL6) strain. PLoS One 2014;9:e102392.

30. Reichenbach A, Bringmann A. Glia of the human retina. Glia 2020;68:768–796.

31. Georgiou M, Fujinami K, Michaelides M. Inherited retinal diseases: therapeutics, clinical trials and end points-a review. Clin Exp Ophthalmol 2021;49: 270–288.

32. Jenkins PM, Hurd TW, Zhang L, et al. Ciliary targeting of olfactory CNG channels requires the CNGB1b subunit and the kinesin-2 motor protein, KIF17. Curr Biol 2006;16:1211–1216.

33. Michalakis S, Reisert J, Geiger H, et al. Loss of CNGB1 protein leads to olfactory dysfunction and subciliary cyclic nucleotide-gated channel trapping. J Biol Chem 2006;281:35156–35166.

34. Michalakis S, Xu J, Biel M, et al. Detection of cGMP in the degenerating retina. Methods Mol Biol 2013;1020:235–245.

35. Koch M, Scheel C, Ma H, et al. The cGMP-dependent protein kinase 2 contributes to cone photoreceptor degeneration in the Cnga3-deficient mouse model of achromatopsia. Int J Mol Sci 2020;22:52.

36. Biel M, Michalakis S. Cyclic nucleotide-gated channels. Handb Exp Pharmacol 2009;191:111–136.

37. Biel M, Zong X, Ludwig A, et al. Molecular cloning and expression of the modulatory subunit of the cyclic nucleotide-gated cation channel. J Biol Chem 1996;271:6349–6355.

Received for publication May 21, 2021;
accepted after revision July 31, 2021.

Published online: August 10, 2021.